Determination of Intermolecular Potentials Using High-Energy Molecular Beams

R. James Cross, Jr.

Department of Chemistry, Yale University, New Haven, Connecticut 06520

Received January 13, 1975

All of chemistry is the result of inter- and intramolecular forces. The forces between the constituent atoms in a molecule determine its structure and stability. The forces between like molecules determine the properties of materials. Given this importance, one might expect, or at least hope, that intermolecular forces are easily obtainable. They are not. There are only a few simple systems for which the intermolecular forces are known accurately over a wide range of distances. We review here one of several methods for measuring intermolecular potentials, that of measuring high-energy (4 eV–4 keV) total cross sections using molecular beams. The results are applicable in the estimation of nonbonding interactions in molecules, in the construction of potential-energy surfaces for reactions, and in a number of spectroscopic applications.

Intermolecular forces are a construct of the Born–Oppenheimer (BO) approximation.[1] The full Schrodinger equation involves a Hamiltonian and wave functions which depend on the position of all N nuclei and all n electrons in the system. The only potentials are the coulomb attractions and repulsions. The BO approximation makes use of the fact that nuclei are much heavier than electrons, and therefore move more slowly. The prescription is to freeze the positions of all the nuclei and then to compute the allowed energies and wave functions for the electrons. Each allowed energy is a function of the $3N$ nuclear coordinates and is one of the potential-energy curves or hypersurfaces for the system. Except for very high-energy scattering (many keV), deviations from the BO approximation occur almost exclusively where two surfaces cross each other or pass close to each other as in an avoided crossing. These deviations are usually best treated as a perturbation on the BO approximation.

After solving the electronic problem to get the potential energy surfaces (usually a difficult or impossible calculation), one must solve for the nuclear motion using the potential-energy surface as the potential in Schrodinger's equation or in Hamilton's or Lagrange's equations in classical mechanics. The bound states in this calculation, if any, are the vibrational and rotational states of the molecule. The shape of the surface near a minimum determines the structure of the molecule and the spacing of its vibrational energy levels. The energy distances between the minimum and the various asymptotes give the various dissociation energies. For a reactive system there is usually an energy barrier between the reactants and products. The height of this barrier is related to the activation energy. The location of the barrier determines other properties of the reaction, such as energy disposal.[2]

There are many quantum mechanical methods of varying accuracy, dependability, and cost for solving Schrodinger's equation numerically for the electronic motion to obtain potential-energy surfaces.[3,4] In many cases there may be no experimental method available, so that even a very crude theoretical calculation may be the best available. Experimentally, one measures either the energy levels or the scattering for the system, and from that information one obtains the potential energy surfaces of interest. If a system has many bound states, spectroscopy is the method of choice. Vibrational and rotational energy levels in gas-phase electronic spectra give much information on both the ground- and excited-state surfaces which, in some cases, is sufficient to obtain extremely accurate potential energy curves. If there are few or no bound states, some form of scattering measurement is usually preferable.

The older forms of scattering experiments were the accurate measurement of transport properties[5] (viscosity, thermal conductivity, diffusion, etc.). Each of the measured coefficients is an average of the differential scattering cross section over scattering angle and incident energy. Recently, the use of molecular beams has made it possible to measure the differential cross section directly.[6] The experiments are generally more difficult, but the results are cleaner and more easily interpreted. There are basically two types of beam experiments, differential and total. In the differential method two molecular beams intersect, usually at right angles. At the intersection the molecules may scatter or react chemically, and the products recoil away from the intersection region with

Professor Cross was born in New York in 1940. He received his bachelor's degree from Yale in 1962 and his Ph.D. from Harvard in 1966. In 1965–1966 he was a postdoctoral fellow at the University of Florida and since 1966 he has been on the faculty at Yale where he is now Associate Professor of Chemistry. His present research includes theoretical studies of inelastic scattering and experimental work on elastic and reactive scattering using molecular beams.

(1) H. C. Longuet-Higgins, *Adv. Spectrosc.*, **2**, 429 (1961). See also J. Tully, *J. Chem. Phys.*, **59**, 5122 (1973).

(2) For a review, see J. Polanyi, *Acc. Chem. Res.*, **5**, 161 (1972).

(3) H. F. Schaefer, "The Electronic Structure of Atoms and Molecules, A Survey of Rigorous Quantum Mechanical Results", Addison-Wesley, Reading, Mass., 1972.

(4) F. T. Smith, "Invited Papers of the Seventh Conference on the Physics of Electronic and Atomic Collisions", North-Holland Publishing Co., Amsterdam, 1972.

(5) J. O. Hirschfelder, C. F. Curtiss, and R. B. Bird, "Molecular Theory of Gases and Liquids", Wiley, New York, N.Y., 1954.

(6) R. B. Bernstein and J. T. Muckerman, *Adv. Chem. Phys.*, **12**, 389 (1967); J. P. Toennies, *Discuss. Faraday Soc.*, 55 (1973).

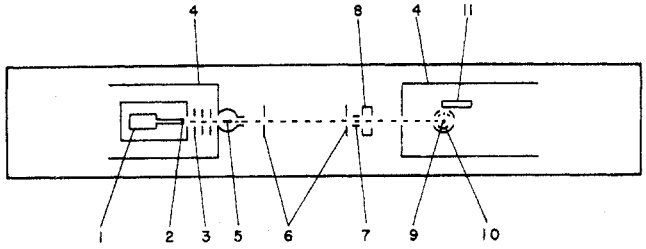

Figure 1. Schematic diagram of the Yale apparatus: (1) alkali oven, (2) heated tungsten plug, (3) ion lens, (4) liquid-nitrogen-cooled cold traps, (5) crossed, neutralizing beam, (6) collimating slits, (7) charged ion deflection plates, (8) scattering chamber, (9) detector (tungsten filament), (10) simple collector plate, (11) electron multiplier.

some distribution in scattering angle relative to the directions of the incident beams; this is the differential cross section $I(\theta,\varphi)$. By rotating a detector about the intersection (or, equivalently, by rotating the sources), one can measure I. By careful control of the distributions of beam velocities and of angular spreads in the beams one can resolve a series of quantum mechanical interferences which, when analyzed, yield very accurate potential-energy curves for atom–atom elastic scattering.

The measurement of total cross sections is simpler. A beam is passed through a scattering chamber, filled with the desired gas, and then detected. The signal at the detector is given by an equation analogous to Beer's law

$$F = F_0 \exp(-nlQ) \tag{1}$$

where F_0 is the intensity when there is no gas in the chamber, n is the number density (concentration) of the scattering gas (molecules/cm^3), l is the length of the chamber, and Q is the total cross section. Q has units of area and may be thought of as an effective target area. Q is related to the differential cross section by

$$Q = \int_0^{\pi} \sin\theta \, d\theta \int_0^{2\pi} I(\theta,\varphi) d\varphi \tag{2}$$

Where both methods are applicable, the differential method is preferred because it gives more detailed information, leading to a more accurate potential. Since the total cross section requires only the detection of the beam and not the detection of scattered molecules, it can be used where the beam intensities are too low for a differential measurement.

In classical mechanics the center of mass[7] (CM) scattering angle θ, the angle between the initial and final relative velocities, is given[6] by a simple integral involving the potential $V(r)$, the relative translational energy E, and the impact parameter b (the distance of closest approach between the two atoms if there were no interaction). The classical CM differential cross section is given by[8]

$$I(\theta) = b|\sin\theta \, \partial\theta/\partial b|^{-1} \tag{3}$$

Quantum mechanics rounds out the singularities at the rainbow angle where $\partial\theta/\partial b = 0$ and at $\theta = 0$ ($b = \infty$) and also provides two types of oscillations at small angles which result from the interference of the scattering from the three impact parameters which contribute to the same θ. As indicated, θ is determined by an integral over $V(r)$; however, the integrand is largest near r_m, the distance of the closest approach, which means that the scattering at angle θ is most sensitive to $V(r_m(\theta,E))$. Not surprisingly, scattering at larger angles and higher energies is sensitive to smaller r (larger V) than scattering at smaller E and θ. Thermal-energy cross sections, both differential and total, are most sensitive to the attractive part of the potential. It is difficult to get thermal differential cross sections in the large-angle region influenced by the repulsive wall of the potential, and, of course, it is impossible via classical mechanics to obtain the potential above the initial relative kinetic energy.

Experimental Techniques

Since chemical bond energies fall well above kT it is important to measure the repulsive part of the potential up to a few electron volts. Data in this region are important in such things as constructing potential-energy surfaces for reactions and in estimating nonbonded repulsions in molecules. Unfortunately, beams in this energy range are difficult or impossible to form. A way out of this dilemma was found by the late Professor I. Amdur at M.I.T.[9] He made neutral beams at much higher energies by charge exchange of ions and used these beams to measure total cross sections. Since the total cross section is sensitive to the scattering at very small angles (minutes of arc), the potential required to effect this scattering is much smaller than the beam energy. Thus a potassium atom at 1 keV may be deflected by an angle of 5′ by a potential of only ~0.5 eV. Total cross sections are not difficult to measure, and, since only small-angle scattering is important, the theory simplifies appreciably. Since Amdur's original measurements, several groups, including the author's group at Yale, have made similar measurements for both ions and atoms.

Figure 1 shows a schematic of the apparatus at Yale,[10] designed to accelerate alkali metals; other apparatuses have a similar design. Alkali vapor is formed in an oven (1) and is ionized in a heated plug of porous tungsten (2). This surface ionization takes place because the ionization potential of the alkali metals is less than the work function of tungsten: the tungsten simply grabs the outer electron and leaves a thermal ion. The process is about 100% efficient for K, Rb, or Cs. The ions are accelerated and focused by an ion lens system (3), a stack of plates with holes in them. After getting the ions to the desired energy they are neutralized by resonant charge exchange in a crossed neutral beam of the same alkali metal (5). When the ion and neutral collide, the outer electron of the atom is naturally attracted to the positive ion and may jump from one nucleus to the other. Such processes take place at large impact parameters with little change in momentum of the nuclei. Conservation of energy and momentum dictate that neutrals traveling in the direction of the ion beam must have very nearly the same kinetic energy as the ions. Hav-

(7) The center of mass (CM) coordinate system has its origin at the center of mass of the two colliding molecules. By conservation of momentum, the LAB velocity of the center of mass does not change. In the CM system the motion of the two molecules can be treated as the motion of a single particle of effective mass $\mu = m_1m_2/(m_1 + m_2)$.

(8) R. B. Bernstein, *Adv. Chem. Phys.*, **10**, 75 (1966).

(9) I. Amdur and J. E. Jordan, *Adv. Chem. Phys.*, **10**, 29 (1966). This is a review of earlier work.

(10) C. J. Malerich and R. J. Cross, *J. Chem. Phys.*, **52**, 386 (1970).

ing produced a high-energy neutral beam, one can then use it for scattering. The beam is passed through a scattering chamber 1 in. long (8) and is finally detected by surface ionization. The beam strikes a fine tungsten wire (9) (0.005 in. in diameter) where it is ionized. The ions are accelerated into the cathode of an electron multiplier (11) which amplifies the beam intensity by $\sim 10^6$. Further amplification is achieved by an electrometer.

Gas is admitted to the scattering chamber (8) from a leak valve to maintain a steady pressure from 0 to 10 μ, enough to attenuate the beam to about 50%. The absolute pressure is measured by a Baritron capacitance manometer which measures the deflection of a thin nickel foil separating two chambers, one connected to the scattering chamber and the other at a high vacuum. The procedure is to keep the beam at one energy and measure the beam intensity as the pressure in the scattering chamber is varied. Using a least-squares fit to (1), the cross section is obtained. This procedure is repeated at many energies to get $Q(E)$. The upper energy limit is determined by breakdown voltages of insulators. It can be as high as 50 keV; in the Yale apparatus it is 1 keV. At energies of several keV the results may no longer be determined by a single potential-energy surface. The lower energy limit is determined by the space-charge blow-up of the ion beam. In the Yale apparatus, when everything is working, and, when all gods and spirits have been properly propitiated, a beam energy of 4 eV can be achieved.

The configurations of other machines measuring high-energy total cross sections are similar.[9] The chief differences are in the sources[11] and detectors.[12] For alkali ion scattering the same source can be used except that the ions are not neutralized. The detector consists of an electron multiplier preceded by a defining slit. Nonalkalis cannot be ionized by surface ionization (or else the efficiency is low). Ions are made by electron bombardment of the neutral gas. Neutralization of the ions is usually done in a chamber rather than a crossed beam. Detection is usually accomplished by a bolometer, which responds to the energy released when the beam collides with it, or an Auger detector, a surface of low work function (such as the cathode of an electron multiplier) which ejects electrons when struck by a high-energy atom. Because the efficiency of formation and detection is less than in the case of alkali atoms, the lowest accessible energy is generally ~ 50 eV.

Interpretation of Results

The actual cross sections measured by the procedure described above are not the true quantum mechanical cross sections given by (2). Even at thermal energy most of the scattering occurs at very small angles such that the scattered molecules may still be detected. Note that (3) gives a nonintegrable singularity in the differential cross section at $\theta = 0$. This is rounded out by quantum mechanics to a finite differential cross section at $\theta = 0$, since it is impossible to distinguish between scattering at very small angles and the broadening of a beam due to the Heisenberg uncertainty in the position and momentum perpendicular to the beam. The fraction of very small-angle scattering increases at high energies so that the experimental cross section, Q_{exp}, may be less than Q by a factor of 4. What is actually measured is

$$Q_{exp}(E) = 2\pi \int_0^\pi I(\theta,E)\mathcal{E}(\theta) \sin\theta \, d\theta \qquad (4)$$

where $\mathcal{E}(\theta)$ is the apparatus efficiency function, the probability that, if a beam molecule is scattered by the CM angle θ, it will be detected as scattered. At small θ, $\mathcal{E}(\theta) = 0$, which makes Q_{exp} less than Q. $\mathcal{E}(\theta)$ is a complicated but easily determined function of apparatus geometry. It was first derived by Kusch.[13] The resolution angle of the apparatus θ_R is given by $\mathcal{E}(\theta_R) = 0.5$; θ_R is approximately d/L where L is the distance between the center of the scattering chamber and the detector and d is the half-width of the beam or detector, whichever is greater. There are two common apparatus geometries: rectangular slit and circular. It is easier to align and construct an apparatus with slit geometry, but the resolution function is more complicated. The Yale apparatus has slit geometry with a resolution of 5.5′. The record is held by Wharton's group at Chicago who have measured thermal cross sections with a circular geometry at 11″ resolution.[14] They could detect the falling of the beam due to gravity.

The procedure for fitting an experimental cross section curve is simply to pick a likely potential, then, using (3) and (4), to calculate the corresponding cross section. The potential is then varied until a satisfactory fit is achieved. The procedure is much less cumbersome than might be apparent. For reasons discussed below, it is not difficult to make a good initial guess. The procedure can be simplified somewhat in the present case of small angle scattering.[10] At low energies (a few electron volts) quantum mechanical effects contribute a few percent. These can easily be included by using a semiclassical method due to Miller.[15] Including quantal effects, it takes only a few minutes of computer time on an IBM 7094 computer to obtain cross sections at 50 energies for an arbitrary potential.

Figure 2 shows a calculated cross section for the Lennard-Jones (6,9) potential

$$V(r) = \epsilon[2(r_m/r)^9 - 3(r_m/r)^6] \qquad (5)$$

ϵ is the well depth, and r_m is the position of the minimum. The energy range is much larger than any experiments. Figure 2 also gives the curve of $b(E)$, the impact parameters which determine the cross section. If quantum mechanical effects are neglected, the inverse-power potential $V = Cr^{-s}$ gives a cross section $Q \propto E^{-2/s}$. The cross sections for each of the terms in (5) taken separately are shown in Figure 2. At high energies, the cross section is determined by collisions with small impact parameters which are governed chiefly by the repulsive wall. At low energies the cross section is determined by three impact parame-

(11) R. K. B. Helbing and E. W. Rothe, *Rev. Sci. Instrum.*, **39**, 1948 (1968).

(12) M. Cavallini, G. Gallinaro, and G. Scoles, *Z. Naturforsch, Teil A*, **22**, 413 (1967); F. J. Van Itallie, L. J. Doemeny, and R. M. Martin, *J. Chem. Phys.*, **56**, 3689 (1972); Y. T. Lee, J. D. McDonald, P. R. LeBreton, and D. R. Herschbach, *Rev. Sci. Instr.*, **40**, 1402 (1969).

(13) P. Kusch, *J. Chem. Phys.*, **40**, 1 (1964).

(14) E. Richman and L. Wharton, *J. Chem. Phys.*, **53**, 945 (1970).

(15) W. H. Miller, *J. Chem. Phys.*, **48**, 464 (1968).

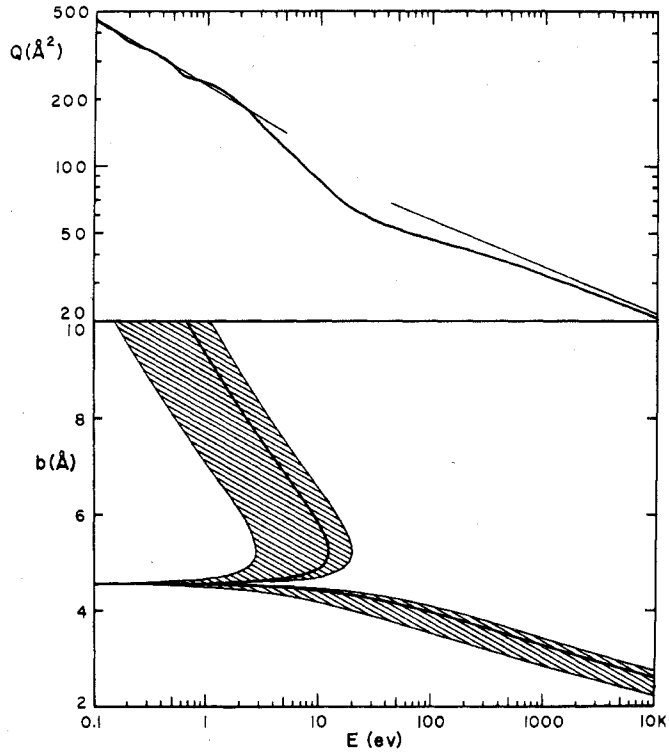

Figure 2. The top curve is $Q_{exp}(E)$ for a Lennard-Jones (6,9) potential with $\epsilon = 9.1 \times 10^{-3}$ eV, $r_m = 4.84$ Å and $\Theta(\theta)$ for the Yale apparatus.[10] The two lines give the cross sections for the limiting inverse sixth- and ninth-power potentials. The lower curve gives the impact parameters corresponding to $\theta = \pm\theta_R$ while the cross-hatched area covers the range of b for $0.1 \leq \Theta(\theta) \leq 0.9$.

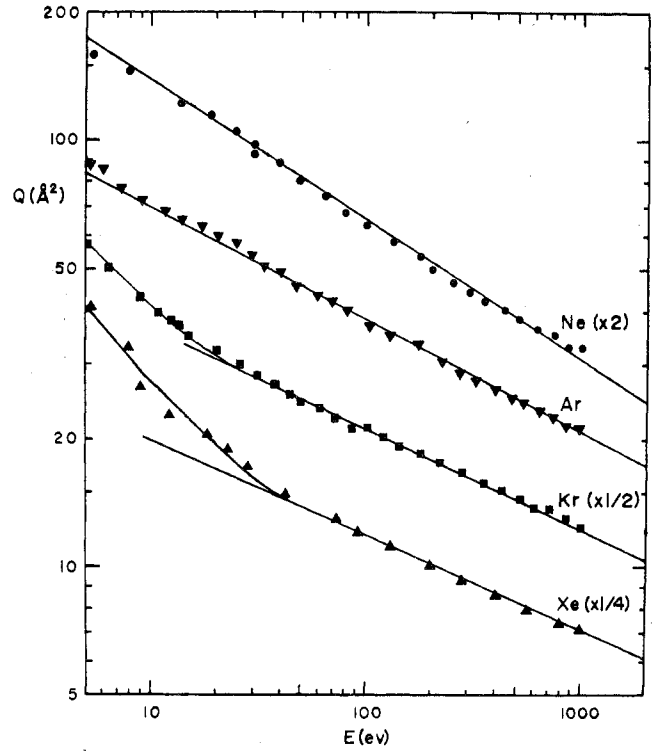

Figure 3. Experimental cross sections for K + Ne, Ar, Kr, Xe. The straight lines give the limiting inverse-power potentials. The curves for K + Kr and K + Xe are the cross sections corresponding to eq 6. See Table II for the potential parameters.

ters, but chiefly by the outermost one. At low energies the scattering is dominated by the long-range attractive branch of the potential. Note that the cross section approaches the limiting high-energy value from below. This is because the actual potential is less than the limiting repulsive potential. That the approach is so slow is a result of the nearly equal range of the two terms in (5). Q rises sharply when the rainbow angle approaches the resolution angle. Here, the classical differential cross section (3) has an integrable singularity ($\partial b/\partial\theta = \infty$). The undulations at low energies are the result of a quantum mechanical interference between the small-angle scattering at large b and the "glory" scattering at smaller impact parameters where the attractive and repulsive forces are nearly balanced.[8] There are two rough scaling laws.[10] For a given potential form, Q is approximately proportional to r_m^2, and the energy scales approximately as $(E\theta_R/\epsilon)$. Thus heavier systems with larger ϵ have the transition between attraction and repulsion at larger energies. Poorer resolution is equivalent to higher energies which, in turn, sample the potential at smaller r.

In deriving a potential from an experimental cross section, one must specify what region of the potential is probed. Q_{exp} is obviously not sensitive to scattering at small angles where $\Theta(\theta) = 0$. Q_{exp} is affected by, but not sensitive to, large-angle scattering where $\Theta(\theta) \approx 1$. A change in $V(r)$ at small r may cause scattering at 50° instead of 30°, but will not affect Q_{exp}. The cross section is determined mainly by scattering at angles for which $\Theta(\theta) \approx 0.5$. As discussed above, this scattering arises chiefly from the potential region near $r_m \approx b$. For the same reasons, Q_{exp} is not affected by electronically inelastic scattering except where it leads to scattering near θ_R.

Results

Space does not allow a thorough discussion of all of the many systems studied to date. Table I gives a list of systems and literature references. These have been confined to measurements of total cross sections in the energy range of 4 eV–4 keV, with some other pertinent results added. Experiments at higher energies involve two or more potential energy curves and electronic excitation. Thermal-energy studies are another large topic in themselves. Recent reviews of these are available.[6]

Alkali metal–rare gas systems have been studied over a wider energy range than other systems because of the ease of ionization by surface ionization. Figure 3 shows the cross sections for K + Ne, Ar, Kr, and Xe from 4 eV to 1000 eV taken on the Yale apparatus. Ne and Ar show only a straight line caused by the repulsive part of the potential. Kr and Xe show the rise caused by the attractive part of the potential as well. In all four cases, as well as in several other alkali metal systems, the repulsive part of the potential can be fit by an inverse-power potential, $V = Cr^{-s}$. The cross sections cannot be fit using an exponential potential, $V = Ce^{-\alpha r}$. The slope of the high-energy cross section directly gives s. Values are in Table II. As is readily apparent, the potentials are soft (small s) in contrast to the popular inverse 12th power potential. This is entirely reasonable given the soft, "squishy" outer s electron on the alkali atom. Another feature is that s depends strongly on the system, varying from 6.0 for Na–Ar to 10.75 for Cs–Xe. This flatly contradicts the law of corresponding states,[5]

Table I
Systems Studied by High-Energy Elastic Scattering

Systems	Ref
Alkali Atom–Rare Gas	
Na + Ar, Xe; K + Ne, Ar, Kr, Xe; Cs + Kr, Xe	10
Cs + He, Ne, Ar	16
Na + Xe; K + Ar, Kr, Xe; Cs + Ar, Kr, Xe	17
Alkali Atom–Miscellaneous	
Li, Na, K, Rb, Cs + Hg	18
Na + Cs	19
K + CH_4, $C(CH_3)_4$, CCl_4, CH_3I, SF_6, N_2, CH_3NO_2	16
Rare Gas–Rare Gas	
He, He	9, 20–22
Ar + He, Ar	9, 23
All pairs except Rn	24
Rare Gas–Miscellaneous	
Ar + O_2, H_2, N_2, CO; He + CH_4, CF_4, CH_3F, CH_2F_3, CHF_3	9
He + H_2	25
H, O, F + He, Ne, Ar, Kr, Xe	24
H + Xe	26
He + H_2, CH_4, N_2O, CO_2; Ne + CO_2; Ar + O_2, N_2	24
N_2O + He, Ne, Ar, Kr, Xe	27
Hg + He, Ne, Ar, Kr, Xe	28
Miscellaneous Neutral Systems	
CH_4 + CH_4; CF_4 + CF_4; CH_3F + CH_3F; CH_2F_2 + CH_2F_2; CHF_3 + CHF_3	9
O + H_2, N_2, O_2, CO, NO, CO_2	24
N + O_2; H_2 + H_2	24
N_2 + N_2, O_2, CO, NO, CO_2, N_2O	24
O_2 + O_2, CO, NO	24
N_2O + N_2O, N_2	27
CO_2 + CO_2, N_2, O_2, CO	27
Alkali Ion–Rare Gas	
K^+ + He, Ne, Ar, Kr, Xe	29–32
Li^+ + He, Ne, Ar, Kr	33
Li^+ + He[a]	34[a]
Li^+ + He[b]	35[b]
K^+ + He[c]	36[c]
Alkali Ion–Miscellaneous	
Li^+ + N_2, O_2[a]	34[a]
Li^+, K^+, Cs^+ + H_2, D_2	37
K^+ + O_2, N_2, CO, NO, CO_2, N_2O	38
Miscellaneous Ionic Systems	
H^+ + He, Ne, Ar, Kr, Xe[a]	28, 40[a]
H^+ + N_2, CO, CO_2, SF_6, H_2, CH_4[a]	40[a]
He^+ + He; H_2^+ + Ar, Kr[a]	40[a]
Cl^- + He, Ne, Ar, Kr, Xe	29
Be^{2+} + He[b]	41[b]

[a] These studies used differential scattering of ions at high energies. [b] Done by an energy loss measurement. [c] This experiment measured large-angle ($\theta \approx 180°$) scattering and therefore sampled the potential at large energies.

which is that a family of chemically similar systems should all have the same potential form, the systems differing only by the scaling factors ϵ and r_m.

In the case of K–Kr and K–Xe we see a different behavior from that seen in Figure 2. In Figure 2 the cross section at high energies slowly approaches the limiting straight line from below. In Figure 3 we see a much more rapid approach from above. This means the potential must approach its limiting form rapidly. Simple addition of attractive and repulsive terms as in (5) does not work. There is no reason to expect that it should. The long-range limit $-Cr^{-6}$ is accurate only at large r ($\geq 3r_m$). Higher order terms proportional to r^{-8}, r^{-10}, etc. are also known. A more general and more realistic form is

$$V(r) = C_s r^{-s}[1 - J(r)] - C_6 r^{-6} J(r) \qquad (6)$$

where $J(r)$ is a joining function which goes from 0 at small r to 1 at large r, thus switching between the attractive and repulsive terms smoothly and continuously. The form of J governs the position and rapidity of the switch.

It should be obvious from Figure 3 that the data are neither sufficiently precise nor extensive to permit an accurate determination of $J(r)$. Indeed, the dependence of Q_{exp} on $V(r)$ in this region is very nonlinear, and thus several potentials might give equally good fits to $Q_{exp}(E)$. Fortunately, K–Kr has been extensively studied at thermal energies so that the potential in the well region and beyond is well known. Düren, Raabe, and Schlier[42] obtained a potential giving a good fit to all the thermal beam data (differential and total). Their potential does not fit the high-energy cross sections, which is no surprise, since none of their measurements depend on the repulsive part of the potential. A fit to this potential gives the joining function

$$J(r) \leq = \exp[-\alpha^2/(r-a)^2] \qquad (r \geq a) \qquad (7)$$
$$J(r) = 0 \qquad (r \leq a)$$

(16) C. J. Malerich, Ph.D. Thesis, Yale University, 1971; C. J. Malerich, K. B. Povodator, and R. J. Cross, unpublished results.
(17) M. Hollstein and H. Pauly, *Z. Phys.*, **196**, 353 (1966); **201**, 10 (1967).
(18) W. Neuman and H. Pauly, *Phys. Lett.*, **22**, 291 (1966); *J. Chem. Phys.*, **52**, 2548 (1970).
(19) W. Neuman and H. Pauly, *Phys. Rev. Lett.*, **20**, 357 (1968).
(20) J. E. Jordan and I. Amdur, *J. Chem. Phys.*, **46**, 165 (1967).
(21) W. J. Savola, E. T. Eriksen, and E. Pollack, *Phys. Rev.* [*Sect.*] *A*, **7**, 932 (1973).
(22) P. B. Forman, P. K. Rol, and K. P. Coffin, *J. Chem. Phys.*, **61**, 1658 (1974).
(23) S. O. Colgate, J. E. Jordan, I. Amdur, and E. A. Mason, *J. Chem. Phys.*, **51**, 968 (1969).
(24) V. B. Leonas, *Usp. Fiz. Nauk*, **107**, 29 (1972) [*Sov. Phys.-Usp.* (*Engl. Transl.*), **15**, 266 (1972)]. This is a review of earlier work.
(25) I. Amdur and A. L. Smith, *J. Chem. Phys.*, **48**, 565 (1968).
(26) M. Picot and R. D. Fink, *J. Chem. Phys.*, **56**, 4241 (1972).
(27) A. P. Kalinin and V. B. Leonas, *Dokl. Akad. Nauk. SSR*, **201**, 53 (1971) [*Sov. Phys. Dokl.*, **16**, 959 (1972)].
(28) T. R. Powers and R. J. Cross, *J. Chem. Phys.*, **56**, 3181 (1972).
(29) I. Amdur, H. Inouye, A. J. H. Boerboom, A. N. v.d. Steege, J. Los, and J. Kistemacker, *Physica*, **41**, 566 (1969); A. Boerboom, H. van Dop, and J. Los, *ibid.*, **46**, 458 (1970).
(30) H. Inouye, S. Kita, and T. Sasaki, *Mass Spectrom.*, **18**, 1177 (1970); H. Inouye and S. Kita, *J. Chem. Phys.*, **56**, 4877 (1972).
(31) I. Amdur, J. E. Jordan, K. R. Chien, W. M. Fang, R. L. Hance, E. Hulpke, and S. E. Johnson, *J. Chem. Phys.*, **57**, 2117 (1972).
(32) F. E. Budenholzer, J. J. Galante, E. A. Gislason, and A. D. Jorgensen, *Chem. Phys. Lett.*, to be published.
(33) H. Inouye and S. Kita, *J. Chem. Phys.*, **57**, 1301 (1972); *J. Phys. Soc. Jpn.*, **34**, 1588 (1973).
(34) W. Alberth and D. C. Lorents, *Phys. Rev.*, **182**, 162 (1964). See also the analysis of Li^+ + He by R. E. Olson, F. T. Smith, and C. R. Mueller, *Phys. Rev.* [*Sect.*] *A*, **1**, 27 (1970).
(35) F. T. Zehr and H. W. Berry, *Phys. Rev.*, **159**, 13 (1967).
(36) H. van Dop, A. J. H. Boerboom, and J. Los, *Physica*, **54**, 223 (1971).
(37) H. Inouye and S. Kita, *J. Chem. Phys.*, **59**, 6656 (1973).
(38) I. Amdur, J. E. Jordan, L. W. M. Fung, L. J. F. Hermans, S. E. Johnson, and R. L. Hance, *J. Chem. Phys.*, **59**, 5329 (1973).
(39) L. D. Doverspike, W. G. Rich, and S. M. Bobbio, *Phys. Rev.* [*Sect.*] *A*, **2**, 2327 (1970); W. G. Rich, S. M. Bobbio, R. L. Champion, and L. Doverspike, *ibid.*, **4**, 2253 (1971).
(40) H. V. Mittman, H. Weise, A. Ding, and A. Henglein, *Z. Naturforsch, Teil A*, **26**, 1112, 1122, 1282 (1971).
(41) W. C. Giffen and H. W. Berry, *Phys. Rev.* [*Sect.*] *A*, **3**, 635 (1971).
(42) R. Düren, G. P. Raabe, and Ch. Schlier, *Z. Phys.*, **214**, 410 (1968).

Table II
Potential Parameters and Ranges for Alkali Metal–Rare Gas Systems

System	Repulsive index, s	Coefficient C_s, eV Å^s	a, Å[a]	α, Å[a]	Potential, r, Å[b]	Range sampled, V, eV[c]
Na + Ar[c]	6.0	101			2.4–4.7	9.4×10^{-3}–0.53
Na + Xe[c]	6.65	360			2.6–5.0	8.1×10^{-3}–0.63
K + Ne[c]	5.75	59.3			2.3–5.6	3.0×10^{-3}–0.49
K + Ar[c]	7.25	618			2.7–5.4	3.0×10^{-3}–0.46
K + Kr	8.0	1900	3.22	1.15	2.9–6.8	-2.8×10^{-3}–0.38
K + Xe	8.5	6190	3.20	0.95	3.1–7.0	-3.0×10^{-3}–0.41
Cs + Kr	10.0	3.52×10^4	3.60	1.15	3.1–6.8	-4.4×10^{-3}–0.43
Cs + Xe	10.75	1.44×10^5	3.90	1.15	3.3–7.6	-3.7×10^{-3}–0.38

[a] The parameters a and α pertain to the joining function defined by (7). For K + Kr they were fit using the potential of Düren *et al.*[42] For the other systems they were fit from the experimental data using (6). [b] The range in r is given by the range in $b(\theta_R,E)$ over the experimental energy range (see text). [c] These systems were fit with a single power-law repulsive potential, $V = C_s r^{-s}$, and hence the range in V is always positive. For the heavier systems the attractive terms were included, and the range in r and V includes the attraction. In these heavier cases s and C_s were fit by the limiting high-energy behavior of $Q(E)$.

A slightly better fit is given by replacing $C_6 r^{-6}$ by $C_6(r - \Delta)^{-6}$. The potential gives a good fit to the data for 3 Å $\leq r \leq$ 7 Å, using Δ = 0.75 Å and C_6 = 241.5 Å;[6] the other parameters are in Table II. The well parameters are: $\epsilon = 9.01 \times 10^{-4}$ eV, r_m = 7.84 Å. The curve in Figure 3 shows the corresponding Q_{exp} for K–Kr. Of the six parameters used in the fit, only two (s and C_s) were determined from the high-energy data; the rest were obtained by a fit to thermal data. Thus there are no adjustable parameters to fit the deviation from the limiting repulsive potential. The agreement with experiment is gratifying. The fit to K–Xe is done completely from the high-energy data using (6–7) with the parameters given in Table II.

Rare gas–rare gas potentials have been measured largely by the Amdur group at M.I.T.[9] and by Leonas et al. at Moscow.[24] Because it is more difficult to ionize a rare gas than an alkali metal, the data were taken at higher energies and do not include the attractive part of the potential. The potentials are smaller than the corresponding alkali rare gas potentials and are harder. Both of these trends are reasonable. The extra s orbital on the alkali atom makes it larger. The orbital contains a single electron, making it easily deformable. The most recent results on He–He[22] agree well with theoretical calculations.[43-46]

A third group of systems that has been well studied are the alkali ion–rare gas systems. These have been studied at high energies by Amdur and Jordan et al. at M.I.T.,[31] Los et al. at Amsterdam,[29] and Inoye and Kita at Tohoku,[30,33] and at lower energies by Powers and Cross at Yale[28] and by Gislason[32] at UICC. The potentials at higher energies resemble the corresponding rare gas–rare gas potentials except that they are somewhat smaller because the electrons are pulled closer to the nucleus by the greater nuclear charge on the alkali metal.[4] At lower energies the potentials are quite different since, at large distances, the ion–molecule potential contains the powerful ion–induced-dipole attraction

$$V_{i-id}(r) = -e^2\alpha/(2r^4) \qquad (8)$$

where α is the polarizability of the atom. This term is much stronger than the van der Waals term and is, of course, absent in the atom–atom case. Low-energy data were fit to potentials of the form of (6–7) except that the attractive term was proportional to r^{-4}.

Recently, Gordon and Kim[47] have developed a simple electron-gas model of the intermolecular potential for closed-shell systems. Their potentials for rare gas–rare gas systems and the high-energy part of the alkali ion–rare gas systems agree quite well with experiment. The agreement with low-energy alkali ion–rare gas potentials is poor. The disagreement is possibly the result of a poor choice of potential function to fit the experimental data. The dependence of the cross section on the potential in the transition region is highly nonlinear, and thus several potentials may fit the data. It is therefore not impossible that the Gordon–Kim potentials may fit the cross section of Powers and Cross.[28] More accurate measurements are now being done by Gislason,[32] so that this discrepancy may soon be resolved.

Conclusion

Our knowledge of intermolecular potentials is slim, but at least we have good knowledge of a few systems over wide ranges. With this we are able to construct reasonable guesses for others. Using various combining rules and simple calculations we can construct guestimates of more complicated potential energy surfaces. Such surfaces are useful in every phase of chemistry from spectroscopy and kinetics to interactions in DNA and proteins.

The author is grateful to the National Science Foundation for the continued support of the research at Yale, to Drs. C. J. Malerich, T. R. Powers, and K. B. Povodator who did the experiments, and to Professors A. L. Smith and R. B. Bernstein for critical readings of the manuscript.

(43) T. C. Gilbert and A. C. Wahl, *J. Chem. Phys.*, **47**, 3425 (1967).
(44) D. J. Klein, C. E. Rodriguez, J. C. Browne, and F. A. Matsen, *J. Chem. Phys.*, **47**, 4862 (1967).
(45) D. Kunik and V. Kaldor, *J. Chem. Phys.*, **56**, 1741 (1972).
(46) N. R. Kestner and O. Sinanoğlu, *J. Chem. Phys.*, **45**, 194 (1966).
(47) Y. S. Kim and R. G. Gordon, *J. Chem. Phys.*, **61**, 1 (1974).